ELSEVIER

Sensors and Actuators A 91 (2001) 363–372

SENSORS AND ACTUATORS A PHYSICAL

www.elsevier.nl/locate/sna

Optical beam steering using MEMS-controllable microlens array

Adisorn Tuantranont*, V.M. Bright, J. Zhang, W. Zhang, J.A. Neff, Y.C. Lee

NSF Center for Advanced Manufacturing and Packaging of Microwave, Optical, and Digital Electronics (CAMPmode), Department of Mechanical Engineering, University of Colorado, Boulder, CO 80309-0427, USA

Abstract

Novel, two-dimensional MEMS-controllable microlens array has been integrated with a vertical cavity surface emitting laser (VCSEL) array using flip-chip assembly. The MEMS/VCSEL hybrid system is built as an efficient and reliable smart pixel array for board-to-board or chip-to-chip optical interconnects in digital systems. Theory including geometrical and Fourier transform analysis and beam steering experimental results are presented. By translating polymer microlens, fabricated on a MEMS *X–Y* movable plate, using electro-thermal actuators, a beam steering angle of 70 mrad is achieved. VCSEL beam steering was successfully demonstrated in our MEMS/VCSEL hybrid system to collimate and steer laser beam for a precision alignment in a two-dimensional free-space optical interconnect.
© 2001 Elsevier Science B.V. All rights reserved.

Keywords: Microlens; Beam steering; Flip-chip; Optical interconnects; MEMS

1. Introduction

Free-space optical interconnection is attractive for several applications including telecommunication switching networks and fine-grained parallel processing/computers. Currently, optical interconnects are used for data communication over long and medium distances in wide area networks (WANs). However, over short distances inside computer systems or clusters of electronic networks, board-to-board or chip-to-chip multi-gigahertz bandwidth optical interconnects are required to replace electrical interconnects in the near future. This replacement is necessary due to problems with signal integrity and crosstalk at high frequency in electrical interconnects. The advantages of free-space holographic interconnects include direct interconnects between boards, arbitrary interconnection patterns, multiple fan-outs, channel isolation and increased bandwidth, thus, avoiding the interconnection bandwidth bottleneck of systems with strictly in-plane electronic interconnects. Furthermore, the cost of free-space interconnects has been reduced substantially with the advancement of vertical cavity surface emitting lasers (VCSELs). However, alignment challenges are inevitable in optical interconnect systems. Mechanical vibrations or thermal expansion can cause misalignment in the systems. In this paper, we present an enhanced alignment approach for free-space interconnects without a demand for tighter assembly tolerances using a MEMS-controllable microlens array. Fig. 1 shows the use of MEMS-controllable microlens array to enhance alignment for efficient and reliable smart pixel arrays on board-to-board optical interconnect in digital systems. The microlens collimates an incident VCSEL beam and the microlens actuators steer the beam to a predefined position on a hologram array by laterally translating the microlens.

Several groups have recently described efforts to steer laser beam using decentered microlens techniques [1,2]. These approaches require light-weight and small travel of the microlens components to achieve agile beam steering. Despite the number of papers on decentered microlens beam steering, all of them seem to require a large space for array of actuators such as comb-drive actuators or scratch drive actuators (SDA) to laterally translate microlens. Moreover, none of them has operated at a VCSEL wavelength of 830 nm because the MEMS devices need to be fabricated on a silicon substrate, which is not transparent at this wavelength. The device presented in our approach contains a dense array of individually controllable microlenses, allowing for operation with a VCSEL array. In this paper, the design, theory, modeling, fabrication, MEMS/VCSEL integration, and experimental results of beam steering are presented.

* Corresponding author. Tel.: +1-303-735-1763; fax: +1-303-492-3498; http://mems.colorado.edu.
E-mail address: tuantran@colorado.edu (A. Tuantranont).

0924-4247/01/$ – see front matter © 2001 Elsevier Science B.V. All rights reserved.
PII: S0924-4247(01)00609-4

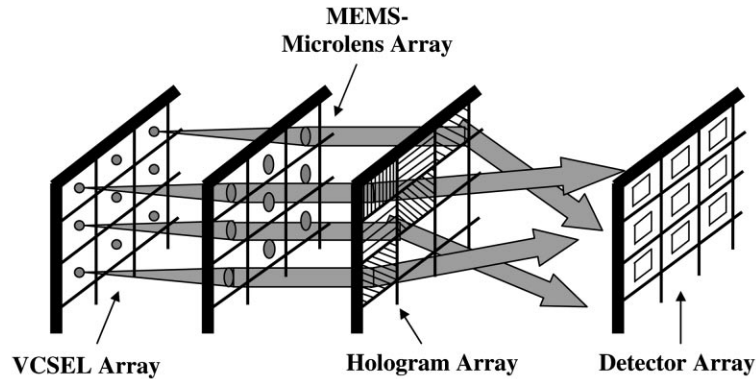

Fig. 1. MEMS-controllable microlens array for enhanced alignment in a two-dimensional board-to-board optical interconnect.

2. MEMS-controllable microlens array device description

The two-dimensional MEMS-controllable microlens array was fabricated through the commercially available surface micromachining technology (Multi-User MEMS Processes (MUMPs)) [3]. Photo-bisbenzocyclobutene (BCB) electronic resin, a photo-sensitive polymer, was used in our own process to fabricate micro semi-spherical polymer lenses on MEMS. Each 120 μm focal length microlens was fabricated directly on a MEMS *X–Y* movable plate with a 30 μm circular aperture as shown in Fig. 2. The microlens was modeled as the thin paraxial lens. The focal length of the microlens is set by controlling the initial thickness of the photo-BCB layer and the diameter of the lens, which are defined by photolithography. The photo-BCB thickness required for a given radius of curvature for the lens was calculated by equating the volume of spherical portion representing the final lens shape to the volume of a cylinder representing the photo-BCB column before reflow [4]. Transmission of microlens is >95% at operating wavelength (850 nm). The lens profile deviates <5% from an ideal spherical lens. Since only a small fraction of lens surface is used to refract light, the effects of spherical aberration and steering-angle-dependent off-axis wavefront aberration are minimized.

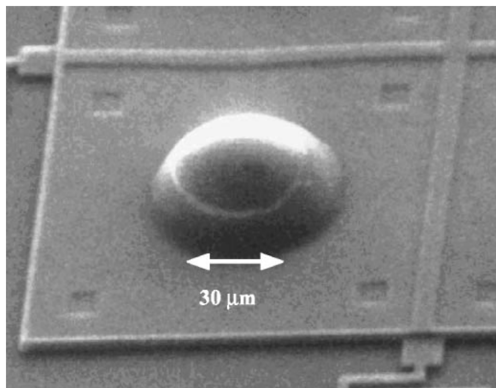

Fig. 2. Polymer microlens fabricated on a polysilicon MEMS movable plate.

Two arrays of electro-thermal actuators are coupled with the 80 μm × 80 μm polysilicon movable plate to translate the microlens in *X–Y* plane. The microlens array is located at a focal plane in front of the VCSEL array and collimates the incident VCSEL beams.

'U'-shaped lateral electro-thermal actuators or 'heatuators' used to drive central plate in a lateral motion consist of a single-material connected narrow arm and wider arm. Current is passed through the polysilicon actuator, and the higher current density in the narrower 'hot' arm causes it to heat and expand more than the wider 'cold' arm. The arms are joined at the free end, which constrains the actuator tip to move laterally in an arcing motion towards the cold arm side [5]. The tips of the actuators are coupled to the central plate by long thin flexures on opposite sides of the plate. Left actuator in Fig. 3, pulls the plate while the right actuator pushes the plate at the same time. By push/pull mechanism of actuators, the motion of the plate is linearly proportional to the consumed power. The mechanical crosstalk in *X*- and *Y*-directions is minimized by using long thin flexures.

3. Theory and modeling of decentered microlens for optical beam steering

The microlens operates in a transmission mode. When the microlens is decentered with respect to the beam axis, the beam will propagate through the off-axis point of the microlens. The microlens still collimates the beam, but the beam is redirected to a nonzero field angle as shown in Fig. 4.

The decentered microlens beam steering is suitable for many agile beam steering applications due to system advantage in terms of weight, beam stabilization, and operating power requirement. The geometrical and Fourier transform analysis of the decentered microlens are described in details.

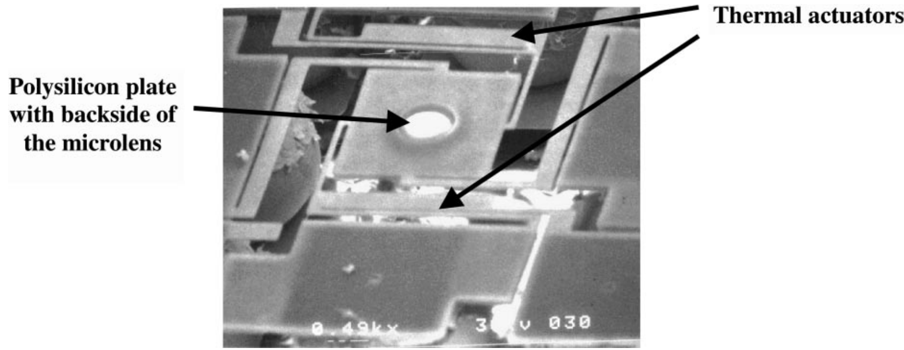

Fig. 3. SEM picture of electro-thermal actuators attached to a suspended polysilicon plate.

3.1. Geometrical analysis

The microlens beam steering device is designed for steering a laser beam of a VCSEL for enhanced alignment in optical interconnect system applications. The output beam from VCSEL diverges as the cone and can be described by a Gaussian beam profile. The laterally translatable microlens was integrated in front of VCSEL with the gap equal to the focal length of microlens, which is in the range of 50–120 μm. Due to the small travel distance of the beam from VCSEL to microlens, we can assume that the beam does not show significant Gaussian beam profile. The steering angle θ depends on the lateral displacement Δd of lens with respect to the beam axis and the focal length f of the lens as shown in Fig. 5. The steering angle is given by [6]

$$\theta = \tan^{-1}\left(\frac{\Delta d}{f}\right) \tag{1}$$

In this scheme, large steering angles are possible by large lens displacement on the order of lens radius assuming a short focal length. The less f-number of lens is, the larger beam steering angle is achieved.

Microlens can be fabricated by using the reflow of polymer technique in post-processing step or using surface micromachining technique to create Fresnel lens. The focal length of the microlens is set by controlling the initial thickness of the polymer layer and the diameter of the lens, which are defined by photolithography. The polymer thickness required for a given lens curvature is calculated by equating the volume of spherical portion representing the final lens shape to the volume of a cylinder representing the polymer column before reflow [4]. The thickness (t) of the polymer necessary to make a spherical microlens focal length (f), radius of microlens (r), dome height of the microlens (h), curvature radius of the microlens surface (R_c), volume of the polymer microlens (V), and index of refraction of polymer (n) are the parameters for the microlens design. The schematic diagram of a lens formed by reflow of polymer is shown in Fig. 6. The paraxial design equations for the polymer microlens are as follows.

The volume of a cylinder of photo-BCB before melting is

$$V = t\pi r^2 \tag{2}$$

The volume of a photo-BCB microlens after melting is

$$V = \tfrac{1}{3}\pi h^2(3R_c - h) \tag{3}$$

The back focal length of microlens is

$$f = \frac{R_c}{n-1} \tag{4}$$

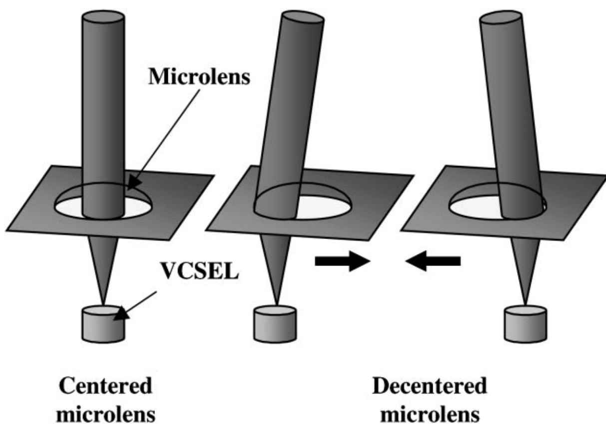

Fig. 4. The decentered microlens concept of MEMS-controllable microlens array.

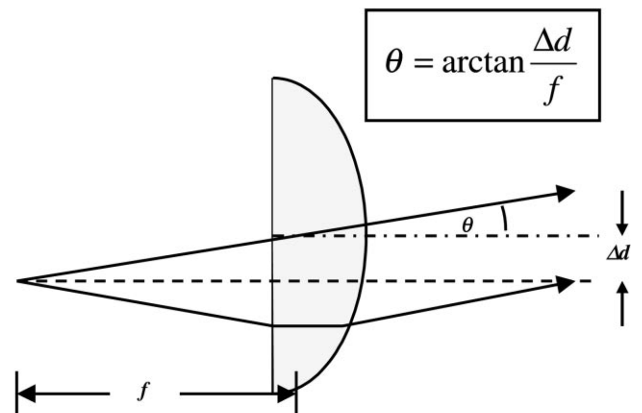

Fig. 5. The steering angle of a decentered microlens.

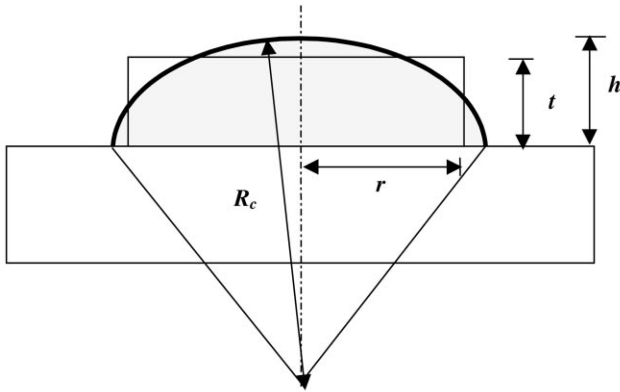

Fig. 6. The schematic diagram of a lens formed by reflow of polymer.

The dome height of microlens after melting is

$$h = R_c - (R_c^2 - r^2)^{1/2} \tag{5}$$

The radius of curvature of microlens surface is given by

$$R_c = \frac{r^2 + h^2}{2h} \tag{6}$$

Finally, the spin thickness of photo-BCB before melting is given by

$$t = \frac{h}{2}\left(\frac{h^2}{3r^2} + 1\right) \tag{7}$$

3.2. Fourier transform analysis

The light from VCSEL is collimated after propagating through the microlens located at the focal length distance in front of the VCSEL. The complex amplitude transmittance of a thin transparent lens [7] is shown in schematic diagram of Fig. 7.

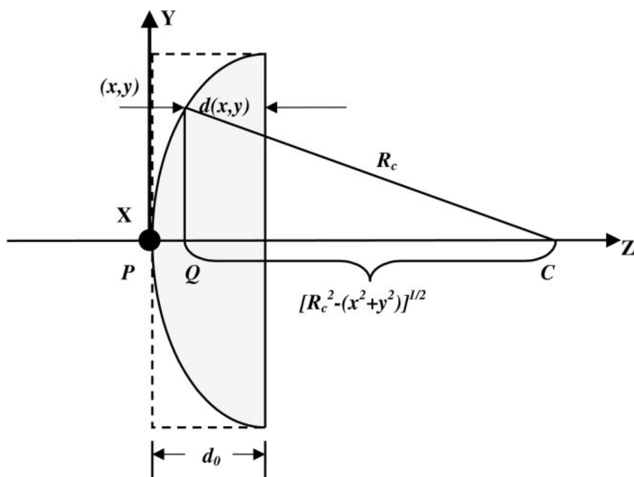

Fig. 7. Schematic diagram of a plano-convex lens.

Since the lens is the cap of a sphere of radius R_c, the thickness at the point (x, y) is

$$d(x,y) = d_0 - \{R_c - [{R_c}^2 - (x^2 + y^2)]^{1/2}\} \tag{8}$$

This expression may be simplified by considering only points for which x and y are sufficiently small in comparison with R_c so that $x^2 + y^2 \ll R_c^2$. In this case

$$[{R_c}^2 - (x^2 + y^2)]^{1/2} = R_c\left(1 - \frac{x^2 + y^2}{{R_c}^2}\right)^{1/2} \approx R_c\left(1 - \frac{x^2 + y^2}{2{R_c}^2}\right) \tag{9}$$

Thus, the thickness at a point x and y is given by

$$d(x,y) \approx d_0 - \frac{(x^2 + y^2)}{2R_c} \tag{10}$$

The incident plane wave continuous to propagate inside the lens as a plane wave with wavenumber nk_0, so that the complex amplitude of the wave $U(x, y, z)$ is proportional to $\exp(-jnk_0 z)$.

Thus, complex amplitude transmittance $t(x, y) = U(x, y, d)/U(x, y, 0)$ is

$$t(x,y) = \exp(-jnk_0 d) \tag{11}$$

In the vicinity of the position $(x, y, 0)$ the incident paraxial wave may be regarded locally as a plane wave traveling along a direction making a small angle with the Z-axis. It crosses the thin lens of width $d(x, y)$ surrounded by thin layers of air of the total width $d_0 - d(x, y)$. In accordance with Eq. (11), the local transmittance is the product of the transmittance of the thin layer of air of thickness $d_0 - d(x, y)$ and a thin lens of thickness $d(x, y)$.

$$t(x,y) \approx h_0 \exp[-j(n-1)k_0 d(x,y)] \tag{12}$$

where $h_0 = \exp(-jk_0 d_0)$ is a constant phase factor.

Substituting $d(x, y)$ from Eq. (10) into Eq. (12), the transmittance of a thin lens is given by

$$t(x,y) \approx h_0 \exp\left[jk_0 \frac{(x^2+y^2)}{2f}\right] \approx h_0 \exp\left[j\pi \frac{(x^2+y^2)}{\lambda f}\right] \tag{13}$$

where $f = R_c/(n-1)$ is the focal length of the lens and $k_0 = 2\pi/\lambda$ is the wavenumber.

The light source in our study is a spherical (or paraboloidal) wave divergent from the VCSEL aperture as shown in Fig. 8. The lens is placed in front of the source at a focal length f. Thus, the beam is collimated and steered after the lens.

We can describe the complex amplitude of spherical beam from source g at x_0 and y_0 coordinates and traveling for distance f as [8]

$$U(x,y) = h_0 G(v_x, v_y) \exp\left[-j\pi \frac{(x-x_0)^2 + (y-y_0)^2}{\lambda f}\right] \tag{14}$$

where $G(v_x, v_y)$ is the Fourier transform of function g of beam from source, $v_x = x/\lambda f$ and $v_y = y/\lambda f$ is the spatial

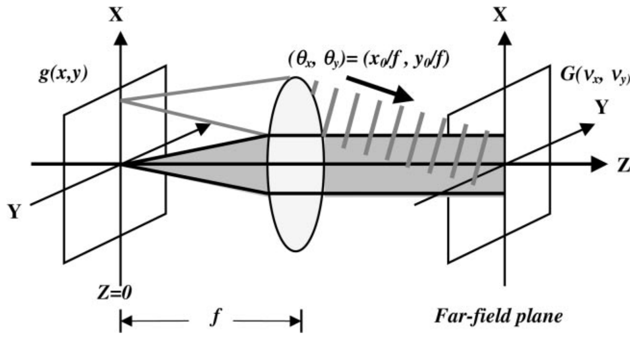

Fig. 8. Fresnel approximation of the far-field waves generated from the off-center point sources at $Z = 0$ plane.

frequency in X- and Y-direction, respectively and $h_0 = (\mathrm{j}/\lambda f)\exp(-\mathrm{j}kf)$ is the phase constant.

Upon the beam crossing the lens, the complex amplitude is multiplied by the lens phase factor from Eq. (13), thus, the far-field complex amplitude is

$$\begin{aligned} U(x,y) &= h_0 G(v_x, v_y)\exp\left[\mathrm{j}\pi\frac{(x^2+y^2)}{\lambda f}\right] \\ &\quad\times \exp\left[-\mathrm{j}\pi\frac{(x-x_0)^2+(y-y_0)^2}{\lambda f}\right] \\ &= h_0 G(v_x, v_y)\exp\left[\mathrm{j}2\pi\left(\frac{xx_0}{\lambda f}+\frac{yy_0}{\lambda f}\right)\right] \\ &\quad\times \exp\left[-\mathrm{j}\pi\left(\frac{{x_0}^2}{\lambda f}+\frac{{y_0}^2}{\lambda f}\right)\right] \end{aligned} \tag{15}$$

Substituting the spatial frequency in X- and Y-direction: $v_x = x/\lambda f$ and $v_y = x/\lambda f$, gives

$$U(x,y) = h_0 G(v_x, v_y)\underbrace{\exp[\mathrm{j}2\pi(xv_x + yv_y)]}_{\text{Plane wave with angle}}\ \underbrace{\exp[-\mathrm{j}\pi\lambda f({v_x}^2+{v_y}^2)]}_{\text{Transfer function of a free-space propagation}},\quad \theta_x = \frac{x_0}{f} = \lambda v_x,\quad \theta_y = \frac{y_0}{f} = \lambda v_y \tag{16}$$

We note that Eq. (16) is the complex amplitude of a plane wave with angle $\theta_x = x_0/f = \lambda v_x$ and $\theta_y = y_0/f = \lambda v_y$ traveling in a free-space. Thus, we can derive the complex amplitude of output beam of the system as the steered plane wave.

3.3. Modeling and finite element analysis

A simulation of the MEMS-controllable microlens was conducted with ABAQUS, which is a commercially available finite element analysis tool [9]. The model consists of an electro-thermal analysis to obtain the temperature distribution resulting from a simulated input power to electrothermal actuators. This is then coupled to mechanical analysis in which the temperature distribution is used to determine deflections resulting from thermal expansion mismatch in hot/cold arms of actuators. The finite element simulation of the temperature distribution in actuators and movement of the plate are shown in Fig. 9.

4. MEMS flip-chip transfer and integration

The procedures for flip-chip transfer of MEMS to a non-silicon substrate (in this case, quartz substrate) need two post-processing steps [10]. First, the MEMS structures are fabricated at a commercial foundry as shown in Fig. 10(a), where a MEMS device is attached to the silicon substrate only by the oxide encasing it. The target substrate is patterned with gold interconnects and bonding pads designed to receive the MEMS structures, as shown in Fig. 10(b). Then, in the second step shown in Fig. 10(c), the two chips are bonded together by thermosonic bonding. Finally, the bonded structure is subjected to a hydrofluoric acid (HF) rinse, as shown in Fig. 10(d), to free the MEMS structure and remove the silicon substrate.

The MEMS-structures were designed and patterned in the first releasable polysilicon layer of the MUMPs process. The photo-BCB microlenses are patterned and fabricated on polysilicon plates by our own process. The plates and actuators are built upside-down on top of sacrificial oxide so that the bonding pads fabricated on MEMS are matched with bonding pads on quartz target substrate. The quartz receiving substrate was patterned with gold wires and bonding pads for MEMS flip-chip bonding and wire bonding. A masked layer of photoresist is used to protect the quartz and gold interconnects when the assembly is released in HF. Gold bumps of 70 μm height are placed on pads and used to bond and electrically connect the MEMS structure and the wiring substrate. The MEMS-controllable microlens array is then flipped and bonded with the wiring quartz substrate using thermosonic bonding. The final step in the process is to release the bonded device in a HF bath and remove the silicon substrate. The final device after flip-chip transfer to a quartz substrate is shown in Fig. 11.

5. MEMS/VCSEL integration

The VCSEL array consists of an 8×8 array of top-emitting VCSELs on a 250 μm pitch. Molecular beam epitaxy (MBE) was used to grow the VCSEL structure on a GaAs substrate. The VCSEL structure consists of two distributed Bragg reflector (DBF) mirrors surrounding a single GaAs quantum well, and is ion implanted for current confinement in the active region. The VCSEL operates at approximately 830 nm with a bandwidth of 0.2 nm and a 2 nm wavelength variation across the array. A Guassian beam with a (e^{-2}) half-angle of 0.135 rad (2 μm in waist) is emitted from the top surface [11]. The threshold current is 1.5 mA. The VCSEL array is flip-chip bonded on a quartz substrate using thermosonic bonding. 90 μm square bonding

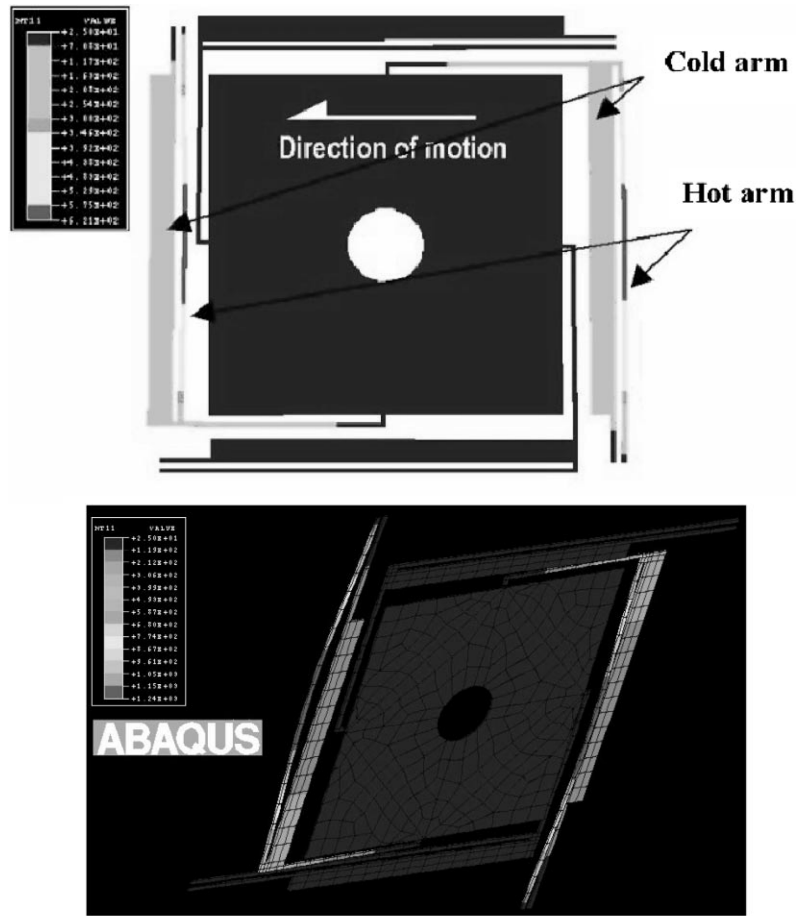

Fig. 9. Finite element simulation of the thermal distribution and movement of electro-thermal actuators.

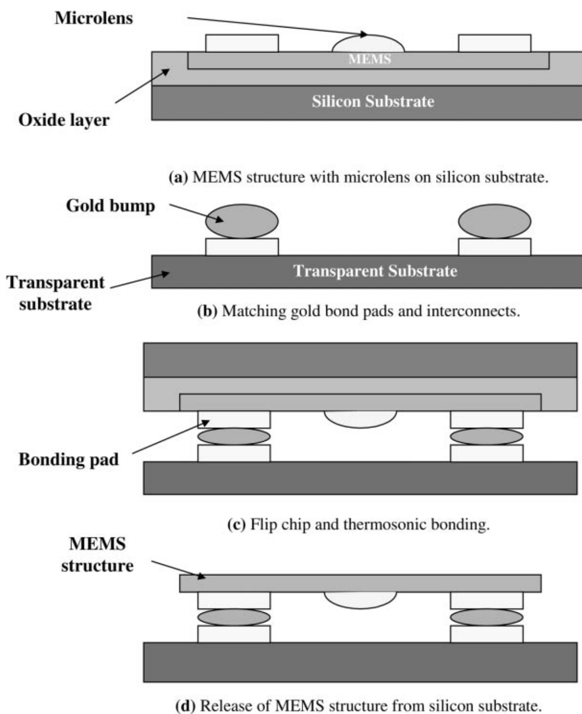

Fig. 10. Flip-chip assembly of MEMS to a non-silicon substrate.

pads for attachment of the flip-chip bonds are evenly interspersed amongst the VCSELs. Each pad is located a distance of 125 μm (center-to-center) from its associated VCSEL. The bonding process uses gold or gold-tin alloy, which is applied to the contacts. The thermosonic bonding method utilizes transverse ultrasonic energy to soften the bonding meterials and uses low temperature (<500 K on the substrate only) and an assembly force ≈0.3 N/bump. A vision assisted, computer controlled placement and assembly machine is used for bonding. Substrate and chip are each centered in separate viewing cameras which allow the relative location of the components to be determined. The substrate is held in a computer controlled translation stage, and the chip is held in a chuck, which is attached to the ultrasonic transducer. The translation stage is used to move the substrate into the aligned position under the chip, and both chips are bonded together. Fig. 12 shows a flip-chip assembled VCSEL array on a quartz substrate with CMOS driving circuit.

Both flip-chip MEMS and flip-chip VCSEL chips are bonded together using UV curable epoxy and aligned under a microscope to correct the lateral misalignment. The optical interferometric microscope is also used to correct the tilt of the final assembly. Then the final assembly is flip-chip

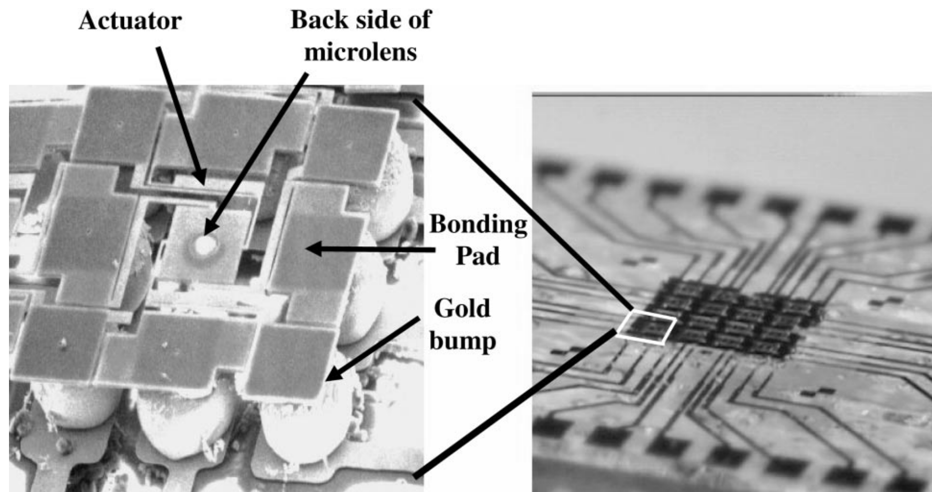

Fig. 11. SEM images of the flip-chip assembled MEMS-controllable microlens 4 × 4 array on a quartz substrate.

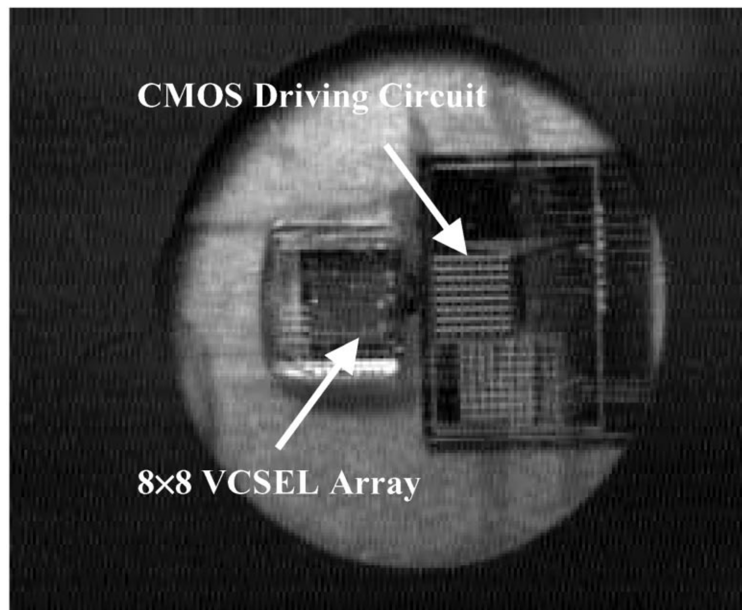

Fig. 12. Flip-chip assembled 8 × 8 VCSEL array on a quartz substrate.

bonded to a ceramic fan-out wiring substrate. The MEMS/VCSEL assembly is then packaged in a 144 ceramic pin grid array (PGA). The schematic diagram of the final assembly is illustrated in Fig. 13.

6. Beam steering experiment and results

CAD program for optical system design, OSLO, was used to simulate the beam steering of the VCSEL beam [12]. The MEMS-controllable microlens array chip was then actively aligned with the VCSEL array chip. First, a decentered Keplerian telescope is used to achieve a collimated beam steering. The controllable microlens is placed at its focal length f_M in front of the focal plane of the lens f_L. The microlens then collimates and steers beam to the desired directions by translating in X–Y plane.

Consequently, the telescope optics, which consist of positive lens ($f_1 = 100$ mm) and negative lens ($f_2 = -50$ mm) are used to magnify the steering angle by the ratio of $f_1/f_2 = 2$. CCD camera was used to detect the deflection of the beams in the far field plane. Fig. 14 shows the Keplerian telescope and telescope lenses in the beam steering experiment setup. The two-dimensional beam steering is successfully demonstrated as shown in Fig. 15.

The maximum beam steering of 70 mrad ($\approx 4°$) is implemented by translating the microlens by one-half of the lenslet diameter as shown in Fig. 16, which is adequate for enhancing optical alignment in free-space optical interconnects. The measured steering angles well agree with the

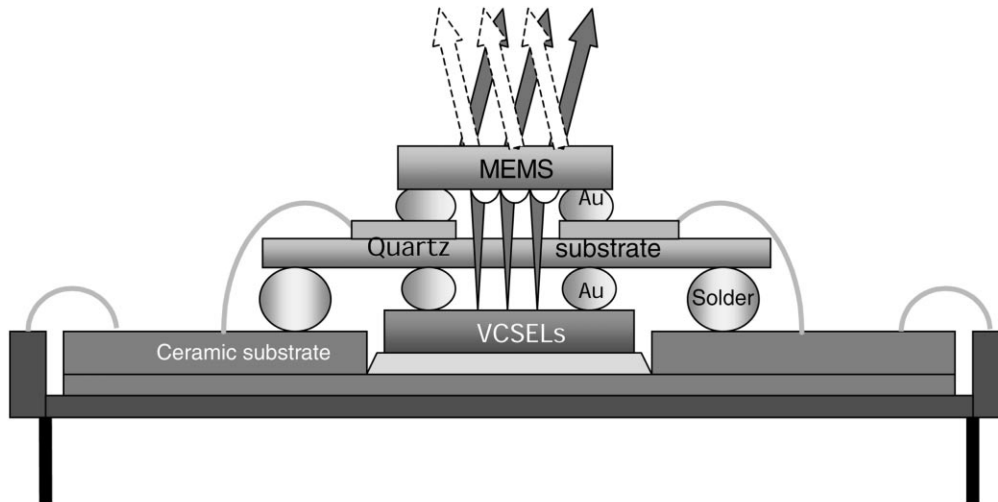

Fig. 13. Schematic diagram of the final MEMS/VCSEL assembly and package.

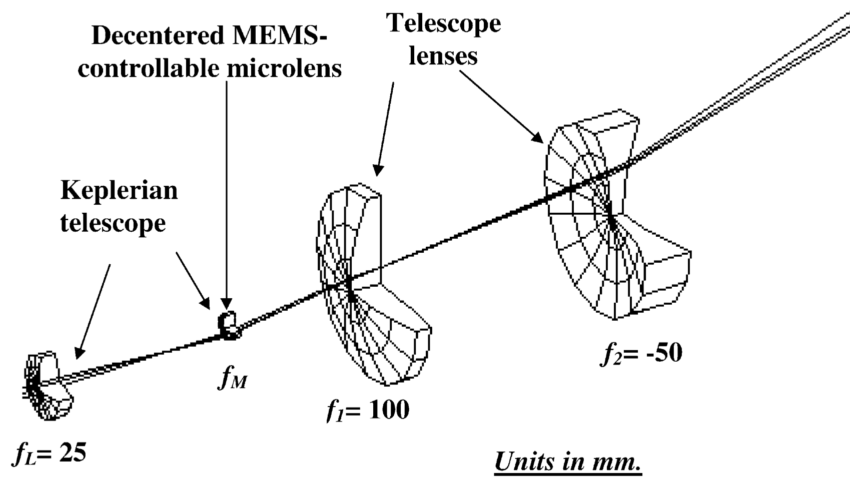

Fig. 14. Optical experimental setup for beam steering demonstration.

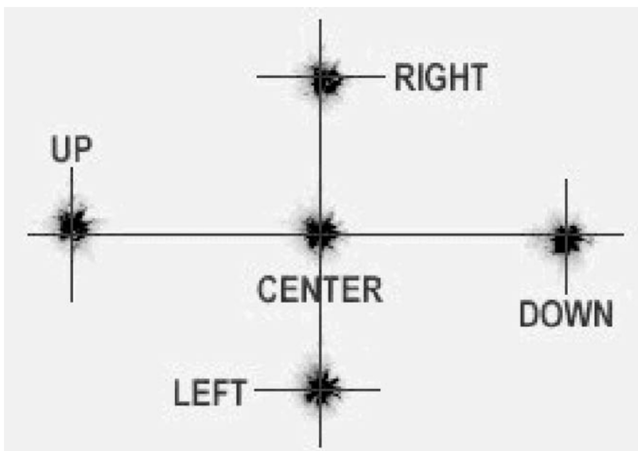

Fig. 15. The two-dimensional beam steering demonstration.

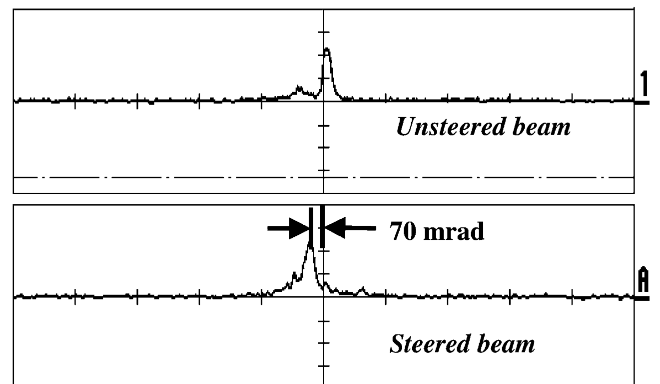

Fig. 16. The maximum beam steering angle of 70 mrad.

theoretical calculation. Measurement verified insertion loss of the system is <2 dB. The system was demonstrated up to a rate of 1 kHz of operation frequency, result of the low inertia and small travel of the microlens components.

7. Conclusions

Novel, two-dimensional MEMS-controllable microlens array has been integrated with a vertical cavity surface emitting laser (VCSEL) array. Theory, modeling and flip-chip integration of MEMS structure on a transparent substrate are described in detail. By translating polymer microlens fabricated on MEMS *X–Y* movable plate using electrothermal actuators, the two-dimensional beam steering is demonstrated and the maximum beam steering of 70 mrad is achieved. VCSEL beam steering was successfully demonstrated in our MEMS/VCSEL hybrid system to collimate and steer laser beam for a precision alignment in a two-dimensional free-space optical interconnect system.

Acknowledgements

This work is supported by the US Air Force Office of Scientific Research (AFOSR), Grant #F49620-98-1-0291. Also thanks to V. Thiantamrong, Li-Anne Liew, and Kevin Harsh.

References

[1] H. Toshiyoshi, J.G. Su, J. Lacosse, M.C. Wu, Micromechanical lens scanners for fiber optics switches, in: Proceeding of the MOEMS'99, 1999, pp. 165–170.

[2] R. Goring, D. Doring, P. Bucker, B. Gotz, P. Chreiber, P. Dannberg, E.B. Kley, M. Cumme, Microoptical concepts for miniaturized scanners and switches from design to realization, in: Proceeding of the MOEMS'99, 1999, pp. 76–87.

[3] D.A. Koester, R. Mahadevan, A. Shishkoff, K.W. Markus, Multi-User MEMS Processes (MUMPs): Design Handbook, Rev. 4, Cronos Integrated Microsystems, 3021 Cornwallis Road, Research Triangle Park, NC 27709, 1999.

[4] A. Tuantranont, V.M. Bright, W. Zhang, J. Zhang, Y.C. Lee, Self-aligned assembly of microlens arrays with micromirrors, SPIE 3878 (1999) 90–101.

[5] J.H. Comtois, V.M. Bright, Surface micromachined polysilicon thermal actuator arrays and applications, Technical Digest of the 1996 Solid-State Sensor and Actuator Workshop, 1996, pp. 174–177.

[6] E.A. Watson, L.J. Barnes, Optical design considerations for agile beam steering, SPIE 2120 (1994) 186–193.

[7] B.E.A. Saleh, M.C. Teich, Fundamentals of Photonics, Wiley/Interscience, New York, 1991.

[8] J.W. Goodman, Introduction to Fourier Optics, McGraw-Hill, New York, 1968.

[9] ABAQUS/Standard User's Manual, Version 5.8, Hibbitt, Karlsson & Sorensen Inc., 1998.

[10] W. Zhang, K.F. Harsh, M.A. Michalicek, V.M. Bright, Y.C. Lee, Flip-chip assembly for RF and optical MEMS, in: Proceeding of ASME InterPack'99, Vol. EEP-26-1, 1999, pp. 349–354.

[11] H.J. Zhou, J. Neff, Y. Chen, V. Fedor, Y.C. Lee, C.C. Mou, W. Berseth, T. Mclaren, E. Tang, Demonstration of a massively parallel bi-directional crosspoint switch with optical control, SPIE 3005 (1997) 266–272.

[12] OSLO, Version 5, Program Reference, Sinclair Optics Inc., 1996.

Biographies

Adisorn Tuantranont received the BS degree in electrical engineering from King Mongkut's Institute of Technology Ladkrabang (KMITL), Bangkok, Thailand in 1995 and the MS degree in electrical engineering (lasers and optics) from University of Colorado at Boulder in 1998. He is now a PhD candidate in Department of Electrical Engineering at University of Colorado at Boulder and works in Optoelectronic Computing Systems Center (OCSC) and Center for Advanced Manufacturing and Packaging of Microwave, Optical and Digital Electronics (CAMPmode). His current research interests include MEM deformable micromirror for optical beam steering and adaptive optics, MEMS-microlens array for optical interconnect, and micromirror for laser resonator and high power application.

Victor M. Bright is an associate professor of mechanical engineering and the director of the MEMS R&D Laboratory, University of Colorado at Boulder. Prior to joining the university, he was an associate professor and the director of Microelectronics Research Laboratory in the Department of Electrical and Computer Engineering, Air Force Institute of Technology, Wright-Patterson Air Force Base, Ohio (6/1992–12/1997). Professor Bright's research includes MEMS, silicon micromachining, microsensors, microactuators, MEMS self-assembly, MEMS packaging, opto-electronics, and semiconductor device physics. Dr Bright received the following awards in the area of MEMS: best paper of the MCM'98 — International Conference and Exhibition on Multichip Modules and High Density Packaging, 1998; R.F. Bunshah best paper award at the 1996 International Conference on Metallurgical Coatings and Thin Films. Dr Bright is a member of IEEE, ASME, and SPIE. He serves on the executive committee of ASME MEMS sub-division.

Jianglong Zhang received the BS degree in engineering mechanics and automation from Tsinghua University, PRC in 1998 and the MS degree in mechanical engineering from the University of Colorado at Boulder in 2000. He is pursuing the PhD degree in mechanical engineering at University of Colorado at Boulder and working in Center for Advanced Manufacturing and Packaging of Microwave, Optical and Digital Electronics (CAMPmode). His current research interests include model of thermal interaction of laser and MEMS and microlens fabrication.

Wenge Zhang received his BSME degree from Dalian University of Technology in Dalian, China, in 1982 and his MS degree in mechanical engineering from the University of Colorado, Boulder in 1995. He joined the University in 1991 and is currently a research associate for the Center for Advanced Manufacturing and Packaging for Microwave, Optical and Digital Electronics, at the University of Colorado. His research interests include low-cost prototyping and thermal management of MCMs, thermosonic flip-chip bonding and optoelectronics packaging. He has 14 years of research experience in mechanical design, computer control systems and logic circuit design and 5 years of research experience in thermosonic flip-chip bonding, MCM substrate fabrication and optoelectronics packaging.

John A. Neff is director of the Optoelectronic Computing Systems Center (OCSC) at the University of Colorado. In addition, Dr Neff directs a research program in optical interconnections for digital systems. Before joining the University of Colorado in March of 1991, he was the research manager for Optical Computing at EI DuPont deNemours & Co., Inc. Prior to joining DuPont in September of 1988, he spent 15 years as a program manager for Optical Computing with the Department of Defense, first with

The Air Force Office of Scientific Research (AFOSR) and then with the Defense Advanced Research Projects Agency (DARPA). At AFOSR and DARPA, he initiated US$ 5 million and US$ 15 million fundamental research programs, respectively, in optical computing. He also spent 4 years as an assistant professor on the graduate school faculty of the Air Force Institute of Technology. He holds a BA degree in physics and mathematics from Ohio Wesleyan University, and MS and PhD degrees in electrical engineering from the Ohio State University. Dr Neff is a fellow of both the Optical Society of America (OSA) and the International Society for Optical Engineering (SPIE).

Yung-Cheng Lee received his BSME degree from the National Taiwan University in 1978, and the MS and PhD degrees from the University of Minnesota, in 1982 and 1984, respectively. Professor Lee is a professor of mechanical engineering and the associate director of the NSF Center for Advanced Manufacturing and Packaging of Microwave, Optical and Digital Electronics, University of Colorado at Boulder. Prior to joining the University in 1989, he was a member of technical staff at AT&T Bell Laboratories, Murray Hill, New Jersey. Professor Lee's research activities include low-cost prototyping and thermal management of multichip modules, three-dimensional packaging, self-aligning soldering, fluxless or solderless flip-chip connections, optoelectronics packaging, microelectromechahical systems (MEMS), and process control using fuzzy-logic models. His teaching activities include design of mechanical components, senior design projects, integrated manufacturing systems, mechatronics, MEMS, robotics, and electronic/optoelectronic packaging.